Stratospheric and Mesospheric HO_x: Results from Aura MLS and FIRS-2

T. Canty[1], H.M. Pickett[1], R.J. Salawitch[1], K.W. Jucks[2], W.A. Traub[1,2], J.W. Waters[1]

T. Canty, Jet Propulsion Laboratory, 4800 Oak Grove Dr, M/S 183-601, Pasadena, CA 91109, USA. (tcanty@jpl.nasa.gov)

[1]Jet Propulsion Laboratory, California Institute of Technology, Pasadena, CA

[2]Harvard-Smithsonian Center for Astrophysics, Cambridge, MA

Observations of OH and HO_2 from Aura MLS for four seasons and diurnal profiles from the FIRS-2 balloon instrument for Fall 2004 are compared with photochemical model simulations testing three sets of kinetics parameters. MLS and FIRS-2 OH profiles, between 25-60 km, are lower than model results using standard kinetics. Use of a faster, previously published rate constant for O+OH leads to better agreement with MLS and FIRS-2 profiles of OH. A 20% increase in the rate of HO_2+OH and the faster rate for O+OH results in improved overall agreement with observations of OH, HO_2, HO_x, and HO_2/OH. Since the MLS and FIRS observations of HO_x are reasonably well described by these models, they are therefore not consistent with the previously reported HO_x dilemma. However, all models considered here result in calculated odd oxygen loss exceeding production, consistent with the long standing ozone deficit problem.

1. Introduction

Simultaneous observations of OH and HO_2 from the Microwave Limb Sounder (MLS) instrument on board the Aura satellite, launched July 15, 2004, provide a unique opportunity to test our understanding of stratospheric HO_x ($OH+HO_2$). We present an analysis of daytime zonally averaged profiles of OH and HO_2 for four seasons using a photochemical model constrained by MLS observations of HO_x precursors. Measurements of OH and HO_2 acquired by the Far-Infrared Spectrometer (FIRS-2) instrument during an Aura validation balloon campaign in September 2004 are also examined.

In the stratosphere, OH is primarily produced through the reaction of water with metastable oxygen, $O(^1D)$, and by water photolysis above 60 km. HO_x is lost primarily through the reaction

$$HO_2 + OH \rightarrow H_2O + O_2. \quad (1)$$

Previous observations of either OH or HO_2 alone have shown poor agreement with model simulations. As a result, two studies have suggested modifications to the rate constants of HO_x partitioning reactions to reach better agreement between measurements and model calculations (see auxiliary material for further discussion[1]). Ground based microwave observations of HO_2 were used to suggest a 60-80% decrease in the rate of

$$HO_2 + O \rightarrow OH + O_2 \quad (2)$$

[*Clancy et al.*, 1994]. Mesospheric OH observations by the Middle Atmospheric High Resolution Spectrograph Investigation (MAHRSI) instrument in November 1994 led to the suggestion of either a 50% reduction in the rate of reaction (2) or both a 20% reduction of rate (2) and a 30% increase in rate (1) [*Summers et al.*, 1997]. However, without simul-

taneous observations of OH and HO_2, it is difficult to attribute the above discrepancies to HO_x loss, production, or partitioning.

These suggested changes were tested against an OH profile measured by MAHRSI in August 1997 [*Conway et al.*, 2000]. Their results showed that the kinetic changes needed to match the MAHRSI OH profile above 50 km led to poorer agreement between modeled and measured OH from 35-45 km. No particular kinetics change allows models to reproduce MAHRSI OH in both the mesosphere and the upper stratosphere. This is known as the "HO_x dilemma" [*Conway et al.*, 2000].

Loss of odd-oxygen (O_x=O_3+O) is dominated by HO_x catalytic processes above 45 km. Ozone, the main component of O_x at these altitudes, should be in photochemical steady state. However, calculated loss of O_x generally exceeds production by ∼35% [e.g. *Jucks et al.*, 1996, *Osterman et al.*, 1997]. This leads to an underprediction of upper stratospheric O_3, commonly known as the "ozone deficit problem".

The kinetics changes suggested by *Clancy et al.* [1994] and *Summers et al.* [1997] lead to good agreement with measured mesospheric HO_2 and OH, respectively, and also largely resolve the ozone deficit problem. These results are driven by a reduction in the rate of (2), resulting in more HO_2, less OH, and slower O_x removal compared to a standard model. In contrast, *Jucks et al.* [1998] suggested the rates of reactions (1) and (2) must both be reduced by 25% to best explain FIRS-2 observations of OH and HO_2. The *Jucks et al.* [1998] kinetics change has a negligible effect on the ozone deficit problem. Below, we investigate the implications of recent Aura MLS and FIRS-2 observations for the HO_x dilemma and ozone deficit problem.

2. Measurements and Model

The Aura MLS instrument measures OH at 2.5 THz and HO_2 at 643 GHz [*Pickett*, 2006]. Validation of MLS OH and HO_2 by comparison with balloon-borne remote sensing measurements of these species is described by *Pickett et al.* [2006].

The MLS profiles presented here are 15 day zonal averages, spanning 34±10°N, centered on September 23 (fall) and December 23, 2004 (winter) as well as March 15 (spring) and June 15, 2005 (summer), based on version 1.51 of the retrieval software. The local solar time (LST) of the observations is ∼13.30 hr. MLS observations of OH, HO_2, HO_x, and HO_2/OH are shown in Figure 1. Here, we only consider data below 60 km, because above 60 km only observations of OH are available [*Pickett et al.*, 2006]. Precision in the 15 day averages for OH and HO_2 is good with negligible uncertainty. The error bars in Figures 1a and 1b are equal to 10%, which represents our estimate of the uncertainty in instrument calibration (i.e., measurement accuracy) [*Pickett et al.*, 2006]. **Raw MLS HO_2 profiles (not shown) exhibit oscillatory behavior that is likely a retrieval artifact [*Pickett et al.*, 2006]. This behavior will result in non-zero reduced chi square (χ^2_r) values even for a model that simulates quite well the overall shape and magnitude of HO_x species. To avoid this situation, we have smoothed the raw MLS profiles of HO_2 using a boxcar average (see auxiliary material [1]) to arrive at the HO_2 profiles used throughout.**

Observations from FIRS-2 were taken by a thermal emission far-infrared Fourier transform spectrometer [*Jucks et al.*, 1998] on board a balloon gondola launched from Ft. Sumner, NM (34.5°N,104°W) on September 23, 2004. These profiles are from ∼1 hour

limb scans. Seven profiles, taken over the course of the day (7:30-17:00 LST), are used for statistical comparison. We consider all data below the balloon float altitude (38 km) and three points above (42, 44 and 48 km) to account for the poorer vertical resolution above float. The OH and HO_2 error bars are the root sum squared (RSS) combination of 1σ estimates of accuracy and precision. Error bars for both HO_x and HO_2/OH shown in Figures 1c and 1d are the RSS propagation of the errors in OH and HO_2 from the respective instruments.

The photochemical model is constrained by MLS measurements of H_2O, O_3, N_2O, CO, and temperature for each season. The model assumes a balance of production and loss for each species integrated over 24 hrs and has been used in previous studies to analyze observations from balloon, satellite, and aircraft platforms [e.g., *Pickett et al.*, 2006, *Jucks et al.*, 1998]. Profiles of Cl_y, NO_y, and CH_4 are specified using well established tracer-tracer relations [*Jucks et al.*, 1998]. The model includes mesospheric chemistry and solar cycle effects, a new feature described in the auxiliary material of *Pickett et al.* [2006].

We show model results for several sets of kinetic parameters: a) JPL02 kinetics [*Sander et al.*, 2003] (hereafter Mdl_{JPL02}); b) same as JPL02 except the *Smith and Stewart* [1994] (hereafter SmSt94) rate constant for O+OH (Mdl_{SmSt}) c) same as Mdl_{SmSt}, except a 20% increase in the rate of HO_2+OH (Mdl_C). The SmSt94 rate constant for O+OH is ∼20% faster than the JPL02 rate and is within the JPL02 uncertainty (Figure 2). The suggested increase in the rate of O+OH is consistent with *Jucks et al.* [1998], who suggested a reduction in k(O+HO_2)/k(O+OH). Two recent laboratory studies of the O+OH rate

89 constant that report contrasting results, published as our work was being completed, are
90 discussed in the auxiliary material[1].

3. Results and Discussion

91 The MLS OH profiles (Figure 1a) all peak near 45 km. Differences in peak values are
92 due to seasonal changes in solar declination. The MLS OH observations and Mdl_{JPL02}
93 calculations result in χ^2_r=12.3, between 25-60 km and considering all seasons (see auxil-
94 iary material[1] for description of χ^2_r; a value of 1 indicates that model profiles generally
95 lie within measurement uncertainty). Mdl_{JPL02} overestimates observed OH between 40-60
96 km, often outside of the measurement uncertainty. Better agreement between modeled
97 and measured OH is achieved for Mdl_{SmSt}. This comparison results in a χ^2_r=3.1 for OH.
98 Results for Mdl_C, described below, lead to a χ^2_r=1.6 (Figure 3). The good agreement
99 between measured OH profiles and the Mdl_C simulation at all altitudes and seasons indi-
100 cates that MLS observations do not exhibit a "HO_x dilemma" as reported by *Conway et*
101 *al.* [2000] for MAHRSI observations of OH.

102 The closest FIRS-2 observations in time (LST=13.6 hr) to the MLS overpass are shown
103 in Figure 1a. The χ^2_r between FIRS-2 observations of OH and the three model cases are
104 larger than for the MLS comparison. The χ^2_r values for FIRS-2 are 16.7 for Mdl_{JPL02},
105 11.8 for Mdl_{SmSt}, and 10.7 for Mdl_C (Figure 4; profiles at seven times have been used to
106 calculate χ^2_r, as described above). These larger values are due to the influence of the
107 higher altitude measurements of OH, which are much smaller than model values. The
108 sense of the discrepancies between FIRS-2 OH and the Mdl_C calculation for September
109 2004 at various altitudes is the same as noted by *Conway et al.* [2000]. However, the

FIRS-2 discrepancies are smaller, particularly near 40 km. The Mdl_C simulation provides a reasonably good description of the shape and abundance of the FIRS-2 OH profile. Hence, the FIRS-2 observations are also not consistent with a HO_x dilemma.

Figure 1b shows comparisons of measured and modeled HO_2. Mdl_{JPL02} overestimates MLS HO_2 **mainly below 40 km**, resulting in a χ^2_r=**2.9**. In contrast to the comparison for OH, Mdl_{SmSt} results in a slightly higher value of χ^2_r (**4.1**) than Mdl_{JPL02}. Best agreement with MLS HO_2 is achieved by Mdl_C, with χ^2_r=**1.7**. The HO_2 profile measured by FIRS-2 is generally higher than observed by MLS (Figure 1b). All three models give excellent agreement with FIRS-2 HO_2 (Figure 4).

We have determined, through a series of sensitivity studies, that a reasonably good overall description of measured OH, HO_2, HO_x, and HO_2/OH is achieved using Mdl_C, which includes a 20% increase in (1) and the SmSt94 rate for O+OH. Profiles of total HO_x and HO_x partitioning from MLS and FIRS-2 are shown in Figures 1c and 1d. The MLS profiles are affected by the oscillations in HO_2. Best agreement between measured and modeled MLS HO_x is found for Mdl_C, with a χ^2_r=**3.0** (Figure 3). For HO_x partitioning (e.g., HO_2/OH) measured by MLS and FIRS-2, the two simulations using the SmSt94 rate for O+OH result in slightly **better** agreement compared to Mdl_{JPL02} (Figures 3 and 4). Considering the suite of model and measured OH, HO_2, HO_x, and HO_x partitioning, represented by "Total" in Figures 3 and 4, Mdl_C kinetics leads to the best overall simulations for both the MLS (χ^2_r=**2.3**) and FIRS-2 (χ^2_r=7.5) data sets, for the suite of model simulations considered here.

If we use the JPL02 rate for O+OH, no simple change to the rate of HO_2+OH improves the simulation of both MLS OH and HO_x in a manner comparable to Mdl_C kinetics. Likewise, it is difficult to reconcile the observations and model results considering only uncertainty in the O+OH rate. The range of model calculations based on the JPL02 uncertainty in O+OH is given in the auxiliary material[1].

4. Ozone Deficit Problem

Calculated (O_x) production (P) and loss (L) rates during Fall 2004, for the three model runs, are shown in Figure 5. Production is the same for all cases because model O_3 has been constrained to the daytime MLS profile. Calculated L exceeds P throughout the upper stratosphere and lower mesosphere, consistent with an ozone deficit problem.

Introduction of the SmSt94 rate for O+OH leads to an increase in calculated HO_2 compared to Mdl_{JPL02}. This increased HO_2 results in larger L-P compared to Mdl_{JPL02} because O+HO_2 is a rate determining step of O_x loss. The Mdl_C simulation results in a value of L-P that is intermediate between the other two simulations above 50 km: the increase in HO_2+OH results in lower HO_x and hence slower O_x loss by all HO_x cycles compared to the Mdl_{SmSt} simulation. A 50% reduction in the rate of O+HO_2 results in balance of P and L near 40 km, as suggested by *Summers et al.* [1997], but leads to poorer agreement with MLS and FIRS-2 HO_x profiles compared to the other simulations shown above (see auxiliary material[1]).

There have been many suggestions in the literature regarding possible resolutions to the HO_x dilemma and the O_3 deficit problem. It has been suggested that reactions involving vibrationally excited $O_2(\nu \geq 26)$+O_2 could solve the ozone deficit problem by providing

an autocatalytic source of O_x [*Miller et al.*, 1994]. However, *Slanger and Copeland* [2003] question the existence of this reactive pathway. *Varandas* [2004] suggested reactions involving vibrationally excited O_2 and OH could be important for both the HO_x dilemma and the O_3 deficit problem. However, *Smith and Copeland* [2005] have raised doubts regarding the suggestion of *Varandas* [2004]. Our observations and simulations, taken at face value, suggest a continued need to resolve the ozone deficit problem without recourse to major perturbations in the kinetic parameters that regulate HO_x.

Acknowledgments. The authors wish to thank G. Smith, L. Kovalenko and B. Drouin for helpful suggestions and discussions. This work was funded by the NASA Upper Atmosphere Research, Atmospheric Chemistry Modeling and Analysis, and Solar Occultation Satellite Science Team programs. Research at the Jet Propulsion Laboratory, California Institute of Technology, is performed under contract with the National Aeronautics and Space Administration. We thank the reviewers for their helpful comments.

[1]Auxiliary material is available via Web browser or via Anonymous FTP from ftp://ftp.agu.org/apend/

References

Clancy, R.T., *et al.* (1994), Microwave observations and modeling of O_3, H_2O, and HO_2 in the mesosphere, *J. Geophys. Res., 99*(3), 5465–5473.

Conway, R.R., *et al.* (2000), Satellite observations of upper stratospheric and mesospheric OH: The HO_x dilemma, *Geophys. Res. Lett.,27*(17), 2613–2616.

171 Jucks, K.W., *et al.* (1996), Ozone productions and loss rate measurements in the middle
172 stratosphere, *J. Geophys. Res., 101*(22), 28785–28792.

173 Jucks, K.W., *et al.* (1998), Observations of OH, HO_2,H_2O, and O_3 in the upper strato-
174 sphere: implications for HO_x photochemistry,*Geophys. Res. Lett., 25*(21), 3935–3938.

175 Miller, R.L., *et al.* (1994), The "Ozone Deficit" problem: $O_2(X,v{\geq}26)+O(^3P)$ from 226-
176 nm ozone photodissociation,*Science, 265*, 1831–1837.

177 Osterman, G.B., *et al.* (1997), Balloon-borne measurements of stratospheric radicals and
178 their precursors: Implications for the production and loss of ozone,*Geophys. Res. Lett.,*
179 *24*(9), 1107–1110.

180 Pickett, H.M. (2006), Microwave Limb Sounder THz module on Aura, *IEEE Trans.*
181 *Geosci. Remote Sensing*, in press.

182 Pickett, H.M., *et al.* (2006), Validation of Aura MLS HO_x measurements
183 with remote-sensing balloon instruments, *Geophys. Res. Lett., 33,* L01808,
184 doi:10.1029/2005GL024048.

185 Sander, S.P., *et al.* (2003) Chemical kinetics and photochemical data for use in atmo-
186 spheric studies, evaluation number 14, *JPL Publ., 02-25.*

187 Slanger, T.G., and R.A. Copeland (2003), Energetic oxygen in the upper atmosphere and
188 the laboratory, *Chem. Rev., 103*, 4731–4765.

189 Smith, G.P., and R.A. Copeland (2005), Comment on "Are vibrationally excited molecules
190 a clue for the O_3 deficit problem and HO_x dilemma in the middle atmosphere?", *J. Phys.*
191 *Chem. A, 109*, 2698–2699.

192 Smith, I.W.M., and D.W.A. Stewart (1994), Low temperature kinetics of reactions be-
193 tween neutral free radicals, Rate constants for the reactions of OH radicals with N
194 atoms (103≤ T/K≤ 294) and with O atoms (158≤ T/K≤ 294), *J. Chem. Soc. Faraday*
195 *Trans., 90* (21), 3221–3227.

196 Summers, M.E., *et al.* (1997), Implications of satellite OH observations for middle atmo-
197 spheric H_2O and ozone, *Science, 277*, 1967–1970.

198 Varandas, A.J.C. (2004), Are vibrationally excited molecules a clue for the O_3 deficit
199 problem and HO_x dilemma in the middle atmosphere?, *J. Phys. Chem. A, 108*, 758–
200 769.

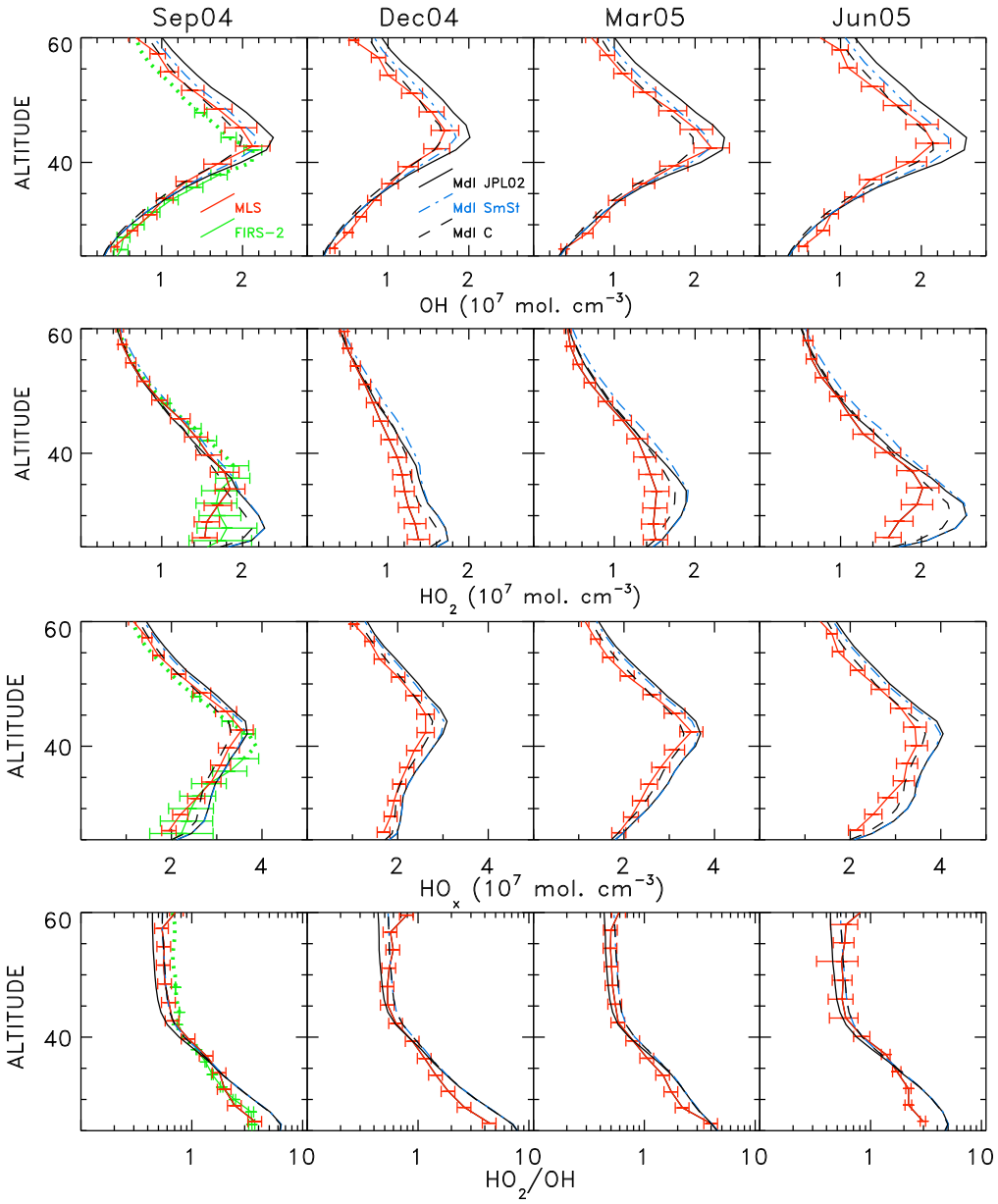
Sep04
Dec04
Mar05
Jun05
ALTITUDE
60
40
MLS
FIRS-2
Mdl JPL02
Mdl SmSt
Mdl C
OH (10^7 mol. cm^-3)
HO2 (10^7 mol. cm^-3)
HOx (10^7 mol. cm^-3)
HO2/OH

Figure 1. 1st Row: MLS OH profiles (red curve) for four seasons and model results for a) JPL02 kinetics, "Mdl_{JPL02}"(black solid), b) *Smith and Stewart* [1994] rate for O+OH, "Mdl_{SmSt}" (blue dashed dot), c) *Smith and Stewart* [1994] rate for O+OH and a 20% increase to OH+HO_2, "Mdl_C" (see text) (black dashed), FIRS-2 observations from Sept 23, 2004 (green curve, data fit to assumed profile shape above float altitude indicated by green dotted curve) are also shown. 2nd Row: same as top row except for HO_2; 3rd Row: same as top row except for HO_x, 4th Row: same as top row except for HO_2/OH.

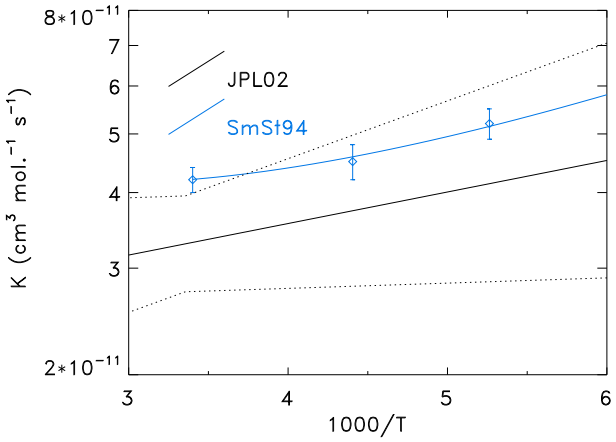

Figure 2. O+OH reaction rate from JPL02 (black) and from *Smith and Stewart* [1994] (blue). Black dotted curves denote uncertainties from JPL02.

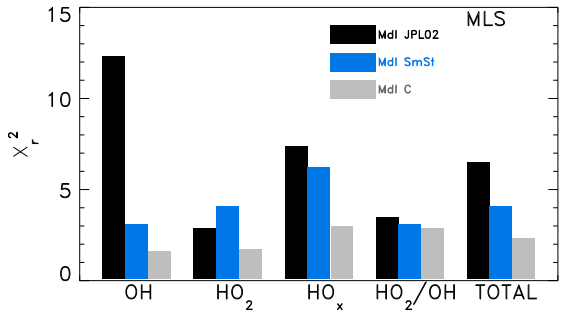

Figure 3. $\chi^2_{\rm r}$ between MLS measurements and: "$\rm Mdl_{JPL02}$" (black),"$\rm Mdl_{SmSt}$" model (blue solid), "$\rm Mdl_C$"(see text) (gray), for OH, HO_2, HO_x, and HO_2/OH. Total represents average of $\chi^2_{\rm r}$ for other 4 parameters.

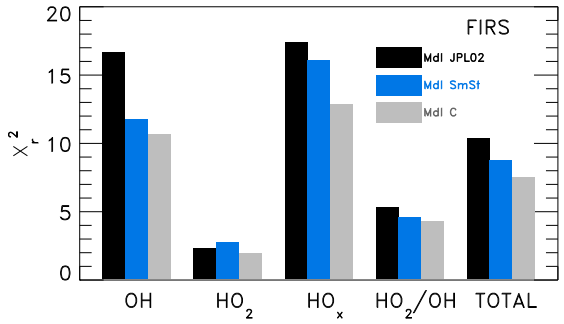

Figure 4. Same as Figure 3, except for comparison of models with FIRS-2 observations

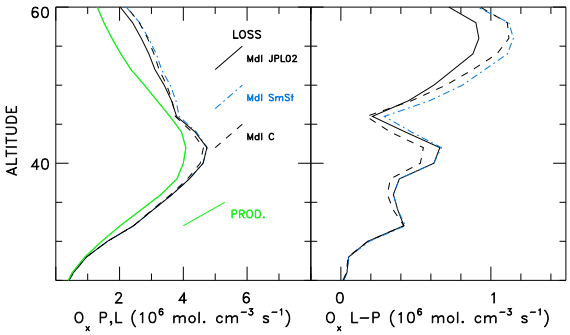

Figure 5. Left Panel: Fall 2004 production (green curve) and loss of odd oxygen from $\mathrm{Mdl_{JPL02}}$ (black curve), $\mathrm{Mdl_{SmSt}}$ (blue dashed dot), and $\mathrm{Mdl_{C}}$ (black dashed), Right panel: Loss-Production of O_x for the 3 scenarios shown in the left panel.

Supplemental Material for Canty *et al.*, Stratospheric and Mesospheric HO_x: Results from Aura MLS and FIRS-2 Manuscript 2006GL025964

$O+HO_2$ Reaction Kinetics

Early studies suggested a large decrease in the rate of the $O+HO_2$ reaction was needed to achieve good agreement between either HO_2 or OH and model calculations [e.g., Clancy et al., 1994, Summers et al., 1997]. The effects of a 50% reduction to the $O+HO_2$ reaction rate, as suggested by Summers et al. [1997] are shown in Figure 6 (Mdl_D). Above 40 km, Mdl_D results in lower OH and higher HO_2 than MLS observations. Below 45 km, Mdl_D OH is lower than than observations from FIRS-2. HO_2/OH calculated from Mdl_D is generally higher than all observations (including errors). A comparison of ${\chi^2}_r$ for Mdl_D (versus MLS data) to values found using MDL_{JPL02} and MDL_{SmSt} is shown in Figure 7. Clearly, MDL_D is less consistent with the MLS observations of HO_x than the other simulations.

As stated in the manuscript, a 50% decrease of the $O+HO_2$ reaction rate does lead to a balance of production and loss near 40 km even though though the calculated profiles of HO_x are not in good agreement with observations (Figure 8).

Box Car Averaging of HO_2 Profiles

As stated in the manuscript, the MLS profiles of HO_2 are smoothed to avoid the oscillatory behavior that is apparent in the HO_2 retrievals shown by Pickett et al. [2006]. Smoothed profiles of HO_2 allow for a more straightforward interpretation of the reduced chi squared analysis (see text). We have applied the following boxcar averaging scheme to remove these oscillations.

$$\sum_{i=1}^{n} HO_2(i) = 0.25\times HO_2(i-1) + 0.5\times HO_2(i) + 0.25\times HO_2(i+1), \quad (1)$$

where i indicates an altitude index. For the HO_2 profile in winter, this box car averaging procedure was applied 3 times to remove an oscillation that was apparent after the previous smoothings. We calculated the endpoints by taking the averaging the endpoint and the next closest point.

O+OH Reaction Kinetics

The range of model calculations based on the recommended JPL02 uncertainties (Sander et al., 2003) from the O+OH reaction is shown in Figure 9 (gray shaded regions). MLS observations of OH above 40 km are often lower than the modeled region though the errors bars overlap. Even with the consideration of the O+OH uncertainties, it is difficult to reconcile the observations with the model results. Calculated HO_2 spans the range of HO_2 observations from the MLS instrument. We again note that the MLS HO_2 profiles exhibit oscillations that may be a retrieval artifact. This behavior is not seen in the FIRS-2 observations. Calculated HO_x ($OH+HO_2$) and partitioning ratios are affected by the high calculated OH. Modeled HO_x is often higher than observations above 40 km. The modeled partitioning ratio is outside of the FIRS-2 error bars through most of the stratosphere.

Two new laboratory studies of the O+OH rate constant, published as our study was being completed, provide contrasting results. The cold temperature study by Carty et al. [2005] suggests a temperature independent rate for this reaction that is 30-50% lower than the JPL02 recommendation, but still within the JPL02 uncertainty (Figure 10). The rate constant measured by Robertson and G.P. Smith [2006] is faster than the JPL02 rate, with a steeper temperature dependence than was seen in any other study (Figure 10). The Robertson and G.P. Smith [2006] rate is similar to the I.W.M. Smith and Stewart [1994] rate for temperatures between 180 and 230 K. At a temperature of 295 K, the Robertson and G.P. Smith [2006] rate is similar to the JPL02 rate. Use of the Robertson and G.P. Smith [2006] rate constant for O+OH results in values of ${\chi^2}_r$ that lie between values of Mdl_{JPL02} and Mdl_{SmSt}, as would be expected by the behavior of the respective rate constants shown in Figure 10.

The laboratory studies of I.W.M. Smith and Stewart [1994] and Robertson and G.P. Smith measured the decay of OH in excess O, monitored by laser induced fluorescence, using experimental setups that were similar. Carty et al. [2005] (I.W.M. Smith is a co-author of this study) also observed the decay of OH by laser induced fluorescence.

However, Carty et al. [2005] used an experimental setup quite different than the other two studies, involving Laval nozzles to achieve extremely low temperature in supersonic flow. Further discussion of the different experimental methods and results is beyond the scope of this paper.

Reduced X_{r}^2

For the statistical results presented in this study, we use a reduced ${X_r}^2$ analysis, where

$$ {X_r}^2 = \frac{1}{\mathrm{N}} \sum_{\mathrm{i}=1}^{\mathrm{N}} \left(\frac{\mathrm{Observation(i)} - \mathrm{Model(i)}}{\mathrm{Overall\ observational\ uncertainty(i)}} \right)^2 \tag{2} $$

A value of unity indicates the model profile is generally within the uncertainty of the observations.

References

Carty, D., A. Goddard, S.P.K. Köhler, I.R. Sims, and I.W.M. Smith, (2005), Kinetics of the radical-radical reaction, $O(^3P_j)+OH(X^2\Pi_\Omega) \rightarrow O_2+H$, J. Phys. Chem., doi:10.1021/jp054429u.

Pickett, H.M., B.J. Drouin, T. Canty, L.J. Kovalenko, R.J. Salawitch, N.J. Livesey, W.G. Read, J.W. Waters, K.W. Jucks, and W.A. Traub (2006), Validation of Aura MLS HO_x measurements with remote-sensing balloon instruments, *Geophys. Res. Lett., 33,* L01808, doi:10.1029/2005GL024048.

Robertson, R., and G.P. Smith (2006), Temperature dependence of O+OH at 136-377 K using ozone photolysis, J. Phys. Chem., doi:10.1021/jp055863z.

Sander, S.P., R.R. Friedl, D.M. Golden, M.J. Kurylo, R.E. Huie, V.L. Orkin, G.K. Moortgat, A.R. Ravishankara, C.E. Kolb, M.J. Molina, B.J. Finlayson-Pitts, (2003) Chemical kinetics and photochemical data for use in atmospheric studies, evaluation number 14, JPL Publ., 02-25.

Smith, I.W.M., and D.W.A. Stewart (1994), Low temperature kinetics of reactions between neutral free radicals, Rate constants for the reactions of OH radicals with N atoms ($103 \leq T/K \leq 294$) and with O atoms ($158 \leq T/K \leq 294$), J. Chem. Soc. Faraday Trans., 90 (21), 3221–3227.

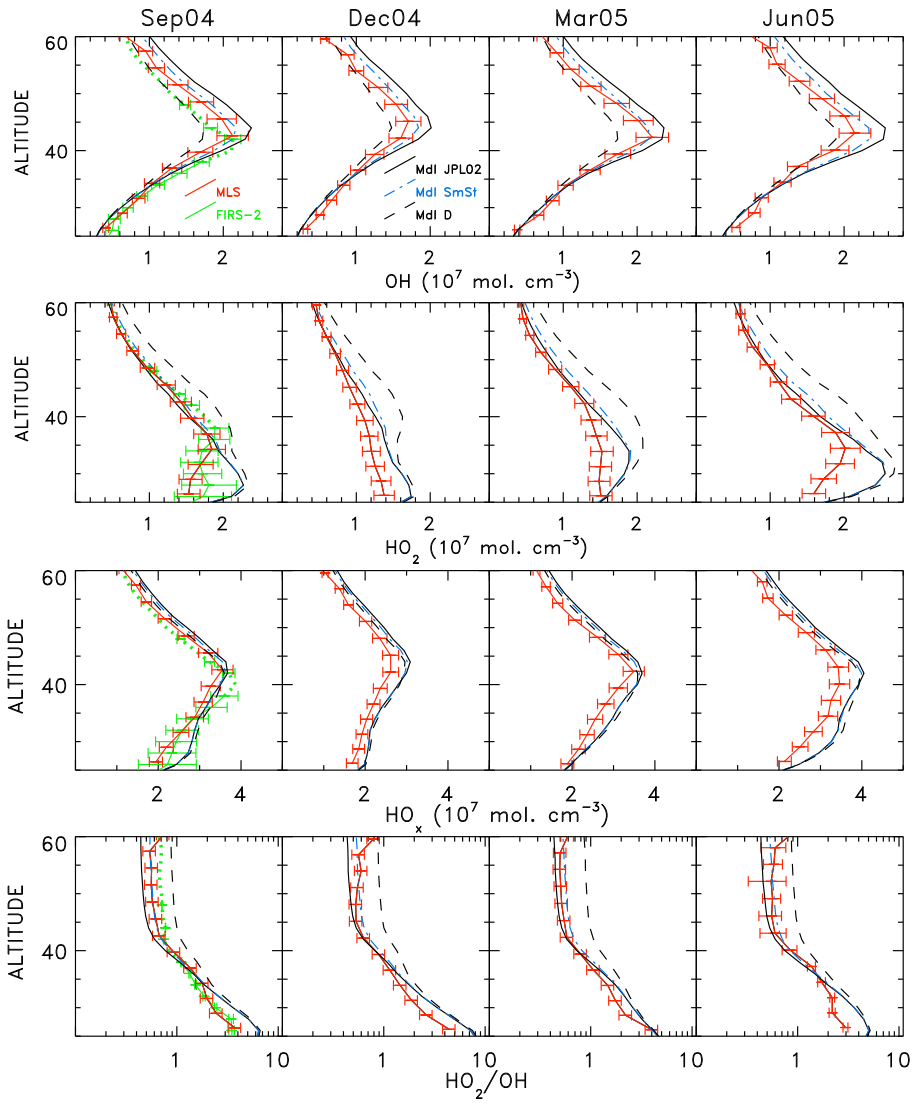

Figure 6. 1st Row: MLS OH profiles (red curve) for four seasons and model results for a) JPL02 kinetics "Mdl_{JPL02}"(black solid), b) reaction rate of O+OH from *Smith and Stewart* [1994], "Mdl_{SmSt}" (blue dashed dot), c) a 50% reduction in the reaction rate of O+HO_2 "Mdl_D" (black dashed), FIRS-2 observations from Sept 23, 2004 (green curve, data fit to assumed profile shape above float altitude indicated by green dotted curve) are also shown. 2nd Row: same as top row except for HO_2; 3rd Row: same as top row except for HO_x, 4th Row: same as top row except for HO_2/OH.

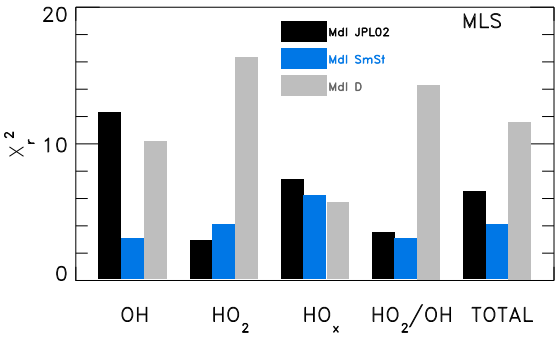

Figure 7. $\chi^2{}_{\rm r}$ between MLS measurements and: "$\rm Mdl_{JPL02}$" (black),"$\rm Mdl_{SmSt}$" model (blue solid), "$\rm Mdl_D$"(gray), for OH, HO_2, HO_x, and HO_2/OH. Total represents average of $\chi^2{}_{\rm r}$ for other 4 parameters.

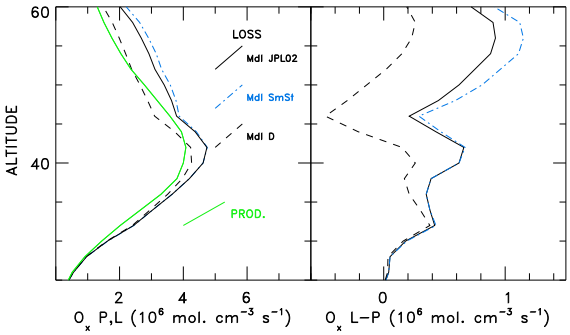

Figure 8. Left Panel: Fall 2004 production (green curve) and loss of odd oxygen from JPL02 kinetics "$\rm Mdl_{JPL02}$" (black curve), reaction rate of O+OH from *Smith and Stewart* [1994], "$\rm Mdl_{SmSt}$" (blue dashed dot), a 50% decrease in O+HO_2, "$\rm Mdl_D$" (black dashed), Right panel: Loss-Production of O_x for the 3 kinetic scenarios shown in the left panel.

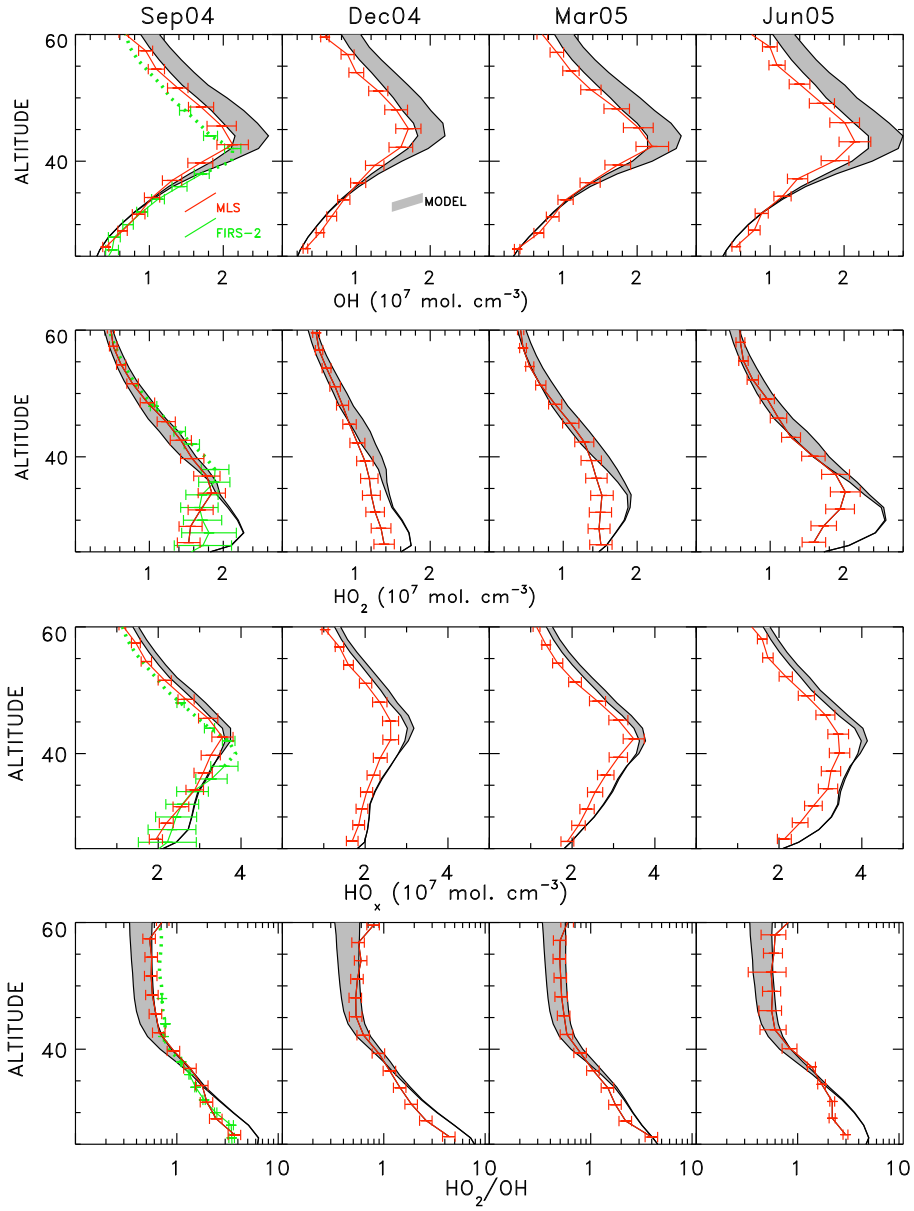

Figure 9. 1st Row: MLS OH profiles (red curve) for four seasons and model results for the recommended JPL02 uncertainty in the O+OH reaction (gray shaded region), FIRS-2 observations from Sept 23, 2004 (green curve) are also shown; 2nd Row: same as top row except for HO_2; 3rd Row: same as top row except for HO_x, 4th Row: same as top row except for HO_2/OH

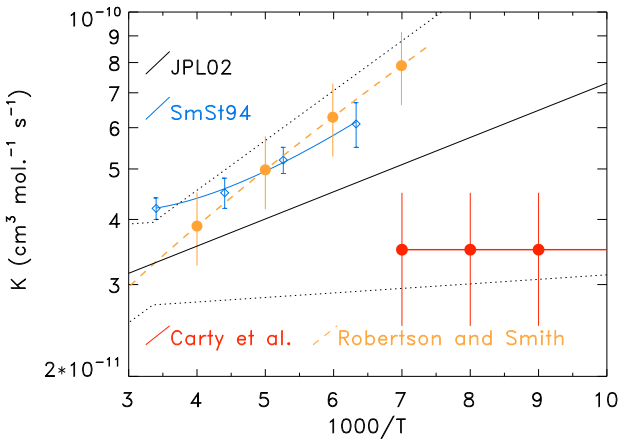

Figure 10. Same as Figure 2 in the main body of the paper, with the addition of rate constants for O+OH measured by Carty et al. [2005] (red) and Robertson and Smith [2006] (orange dashed). Uncertainties for the Robertson and Smith [2006] rate constant represent are 16%, representing the 1σ overall uncertainty stated in their Conclusions section. The uncertainty for Carty et al. [2005] is the value given in their abstract, which applies to all temperatures of the experiment (39-142 K), and represents a combination of the statistical differences of various runs combined with other sources of systematic error.